ISSN: 0067-2904

Experimental Study of Pulsed Electrical Discharge in Cylindrically-Tipped of Plasma Switch

Ala' F. Ahmed*[1], A. S. Hasaani[2]
[1]Department of Astronomy & Space, College of Science, University of Baghdad, Baghdad, Iraq.
[2]Department of Physics, College of Science, University of Baghdad, Baghdad, Iraq.

Abstract
In this research pulse high voltage circuit was used including resistance, inductance and capacitor to achieve an experiment of cylindrically-tipped of plasma switch .The charging voltage of up to 9kV using Rogowski coil and current-shunt resistance (CVR) used to measure pulsed electrical discharge (PED). The current in both self-triggering and third-electrode triggering modes. The pulsed current peaks 4kA and the duration of circuit pulses were recorded between 0.1μs and 0.3μs. The experimental results has shown clearly the inductance effect in the circuit parts in under damped oscillation regarding the value of circuit parts in addition to the distance of the spark gap cylindrically-tipped electrodes during the plasma propagates under air pressure with their circuit impedance. Under the range of experimental states (2-30)Ω nominal impedance ranges were recorded, rely on the gap and circuit parameters.

Keywords: Pulsed electrical discharge, Impedance characteristics, high voltage plasma.

دراسة تجريبية للتفريغ الكهربائي النبضي في مفتاح البلازما الإسطواني المستدق

آلاء فاضل احمدالراشدي*[1]،عبد الرضا سلمان حساني[2]
[1]قسم الفلك والفضاء، كلية العلوم، جامعة بغداد، بغداد، العراق.
[2]قسم الفيزياء، كلية العلوم، جامعة بغداد، بغداد، العراق.

الخلاصة
في هذا البحث تم استخدام دائرة تعمل بفولتية نبضية عالية مكونة من مقاومة ومتسعة ومحاثة لعمل تجارب تفريغ كهربائي في مفتاح بلازماعلى شكل قضيب اسطواني مستدق حيث استخدمت فولتية الشحن فيها الى اكثر من 9 kV .
ولقياس تيار التفريغ النبضي أستخدمت مقاومة مجزئ وملفات روغوفسكي ،عند انهيار مفتاح البلازما بنمطين هما التفريغ الذاتي و باستخدام قطب ثالث للتفريغ حيث كانت قيمة الذروة للتيار 4kA و زمن النبضة تراوحت بين 0.1 μs و 0.3 μs بالاعتماد على مكونات الدائرة والمسافة بين الاقطاب .
حيث لوحظ ظهور سلوك حثي سائد في الدائرة معتمدا على قيمة مكوناتها وخصائص البلازما المتولدة بين قطبي فجوة المفتاح وتاثير ذلك على ممانعة الدائرة النبضية . وفي هذه الظروف التجريبية المعطاة وجد ان القيمة المطلقة للممانعة تتراوح بين 2 اوم و30 اوم معتمدة على حالت التذبذب وطريقة دراسة وتحليل نتائج اشارات تيارالتفريغ الكهربائي.

1. Introduction

Closing plasma switches are "open" naturally and are "closed" with an application of external trigger or as a result of its own over voltage [1]. Different high voltage switches have been used as

*Email: ala.fadil77@gmail.com

key components to transfer electrical energy from the storage unit to the load [2]. Plasma switches are among these switching devices, which can potentially transport high electrical currents at relatively low power dissipation with controllable repetition rate. These plasma switches cover thyratrons, pesudospark, and spark gaps [3-5].

Because of their simple design and construction, low cost, and capability of current level control, spark gaps have stimulated interests in a number of research activities [6-11]. In these studies, a number of operating parameters was investigated including repetition rate, discharge region of operation, electrode erosion, gas pressure, and damping conditions of the output signals [11].

Spark gap switches working in high-pressure gas such as air and nitrogen have been very widely used in high- power pulsed technology. They are known to permit very large currents (hundreds of kA to MA), to have a short current rise time of a few nanoseconds. In comparison with other switches, the main advantages of spark gap switches are a high voltage, large conducting current, high energy efficiency, low cost [12].

In addition, Paschen curve for air with the fixed gap width of 3 mm is overlaid as reference to the breakdown voltage of gaseous media. As seen in Figure-1, all the plasma switches operate below the Paschen curve [13]. Above this curve, the normal operating voltage will exceed the breakdown strength of the gaseous, and will cause unexpected breakdown events [12, 14].

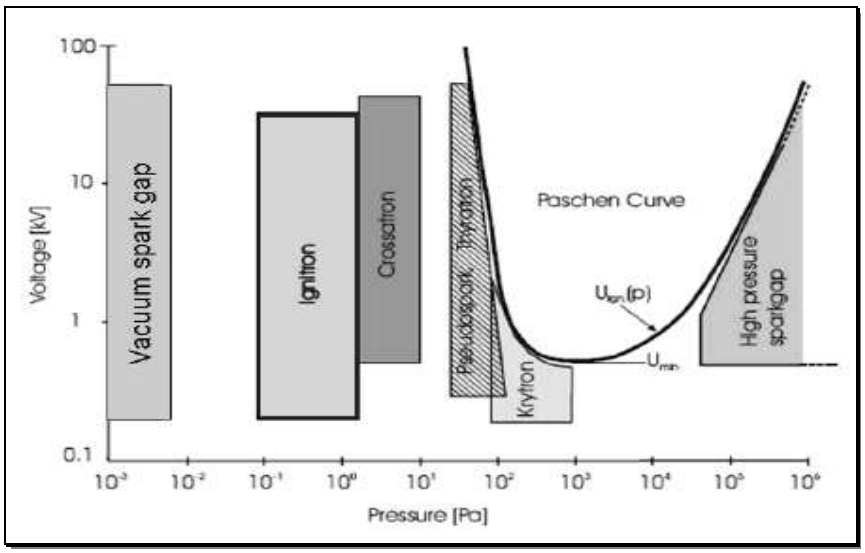

Figure 1- Rang of gas pressures and operating voltage for plasma switches [14].

Nearly all types of plasma switches are operated on the basic principle of ionization and breakdown of gases. Under normal conditions (below its breakdown voltage), gas is an insulator and becomes conducting when ionized [1].

At particular gas pressure P and electrode spacing d, the product pd is known as the sparking parameter and is characterized by the Paschen curve for each gas and geometry [7]. The mechanism involves the production of plasma and the propagation of plasma particles between the electrodes of the spark gap giving rise to a high current flow through the circuit. Characteristic current-voltage curves can then be deduced from the output signals after recording the charging voltage of the capacitor or the energy storage unit.

2. Experimental Setup

A pulsed high-voltage circuit has been designed and constructed to include three main components; inductances, capacitors and resistances. One of the main objectives of this work is to investigate the temporal behavior of the impedance of an atmospheric pressure spark gap for cylindrically-tipped, electrodes at air atmospheric pressure. Analysis of the discharge current oscillograms under various damping conditions was carried out as two triggering techniques were followed after being designed for these experiments. In addition, Rogowski coils have also been designed to measure the current pulse as well as current shunt resistors for comparison.

The measurements were rounded to a proper degree of precision within the capability of the instrumentations providing that pulsed parameters could not be precisely controlled in terms of reproducibility of shot-to-shot output signals.

2-1. Capacitors Bank

High voltage capacitor consists of 16 big size chemical capacitors type, each one with a length of 60 cm, width 34.5 cm and thickness 12.5 cm as shown in Figure- 2. All are connected in parallel to obtain the total capacitor C_{total}= 39 μF. Each accepts the maximum voltage is 30 kV. The stored energy can be calculated for each capacitor by the following relationship:-

$$E = \frac{1}{2} C V^2 \quad \text{……(1)}$$

The maximum energy storage in the capacitor bank is E = 17.6 kJ

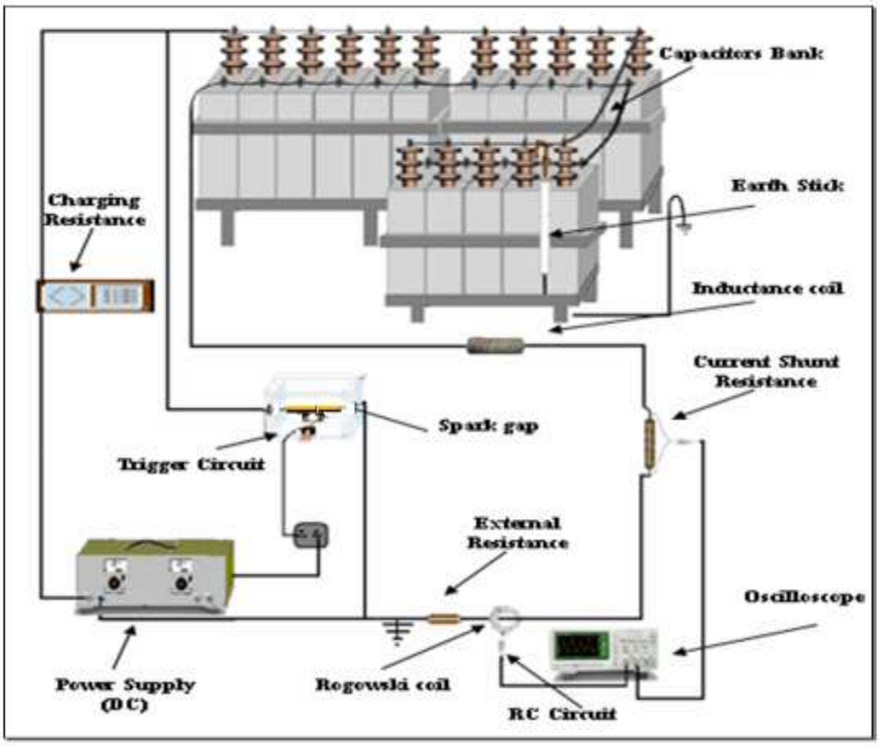

Figure 2- Experimental setup Schematic photograph of the pulsed RLC circuit.

2.2. Cylindrically-Tipped Spark Gap

The cylindrically-tipped spark gap electrode is made of Copper. The measurement of each of the two electrodes:- the ground electrode internal and external radius are r_1=9 mm, r_2 =9.5 mm respectively. The thickness equals 0.5 mm and the length is 46 mm while the high voltage electrode, the internal radius is r_1 = 9 mm and external radius is r_2 = 9.5 mm, thickness equals 0.5 mm and the length is 76.5 mm. This is shown in Figure- 3.

In these experiments, a spark gap with a cylindrically-tipped electrode was incorporated within the high-voltage circuit to establish a good understanding of the geometry effect which may alter the values of the current density rather than the peak current.

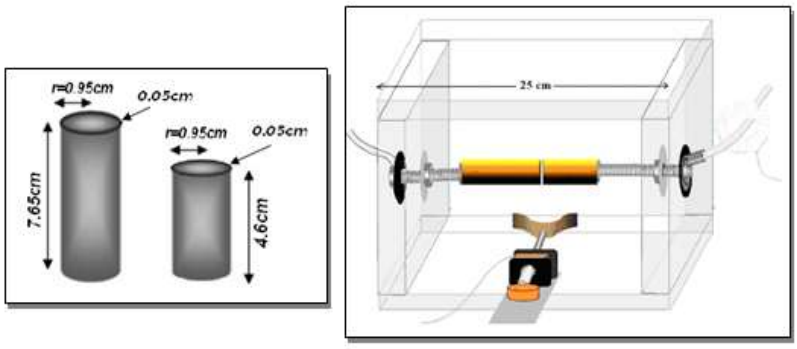

Figure 3- Spark gap schematic for Cylindrically-Tipped.

The cylindrically-tipped electrodes were used in this experiments to form a spark gap as shown in the photograph of Figure- 4 during a typical breakdown stage after a number of shots.

A number of experiments were carried out with this configuration by using both self-breakdown and trigger-electrode modes. By doing so, the effect of an external inductance possessed by the triggering electrode circuit can be observed in the output signal after the circuit is being discharged.

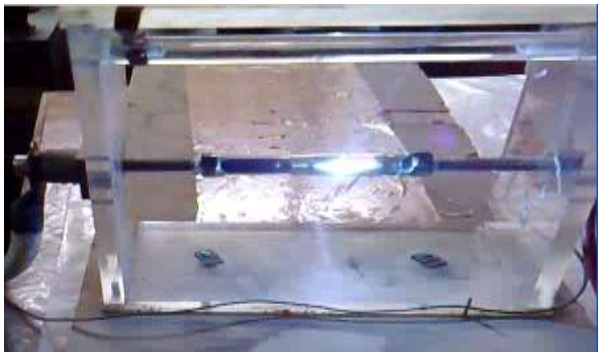

Figure 4- Cylindrically-tipped electrodes during a typical self- breakdown stage.

3-Result and Desiccation:

3-1. Current-Voltage Characteristics Curves

A typical discharge current-charging voltage characteristic curve is shown in Figure- 5 where both CVR and Rogowski coil measurements of the current are demonstrated for triggering mode (third electrode).

The effect of the electric field lines on the applied voltage may be significant and can be altered when the degree of uniformity is considered. This can be simply understood from the basic relationship between the voltage and the electric field for any two electrodes. This degree of field uniformity may be determined by the ratio of the electrode dimension and the gap spacing. In Figure- 6 a typical discharge current–charging voltage characteristic curve for triggering breakdown is shown where both CVR and Rogowski coil measurements of the current are demonstrated. Typical peak current values ranged from 0.8 kA to 4.7 kA were recorded when voltages between 1 kV and 9 kV respectively were applied for changing the C-bank

.

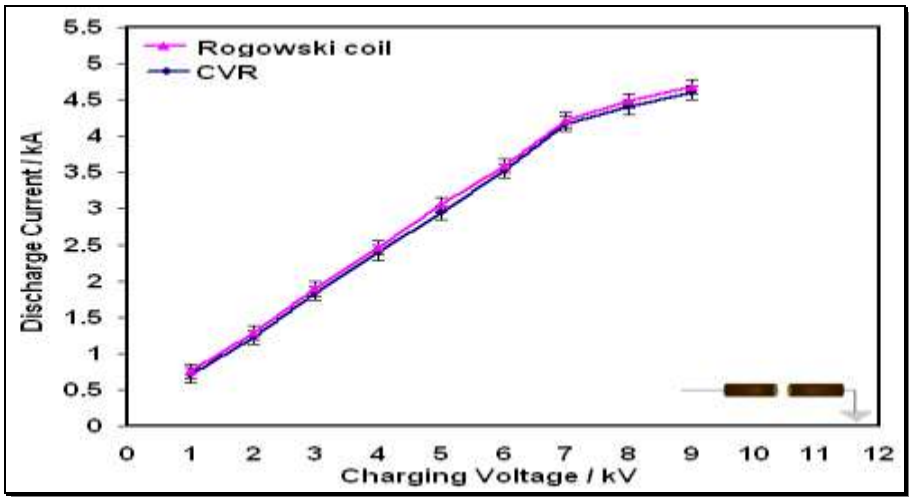

Figure 5- Typical discharge current-charging voltage characteristic curve for d=2mm under third-electrode triggering mode

Although the discharge mechanism is governed by a streamer, such behavior looks linear in a part of it because the voltage considered is the charging voltage. However, more future measurements of discharge voltage may put forward more understanding of the current-voltage characteristic curves.

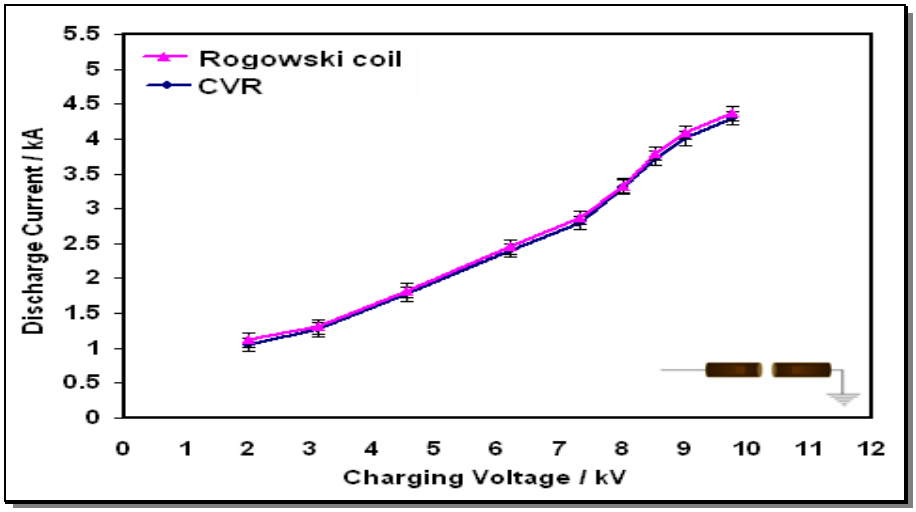

Figure 6- Typical discharge current-charging voltage characteristic curve for different distance at self breakdown.

Comparison of Figures-5 and 6 may significantly present the values of the parameters corresponding to the two modes of triggering the spark gap.

3-2. The Performance of the PED Circuit

Similarly, a graphical representation of the charging and discharging times is shown in Figure- 7. The performance of the pulsed circuit may be envisaged by the ratio (discharging time/charging time) for self-breakdown condition. The differences in current values may be imposed by the (inductance/resistance) ratio of Rogowski coil, which is reasonably acceptable in pulsed techniques. In the present experiments, a peak discharge current of 1 kA was found to have a rise time of 163 ns while increasing current up to 4.3 kA was recorded with a rise time of 174 ns for the CVR measurements at self-breakdown.

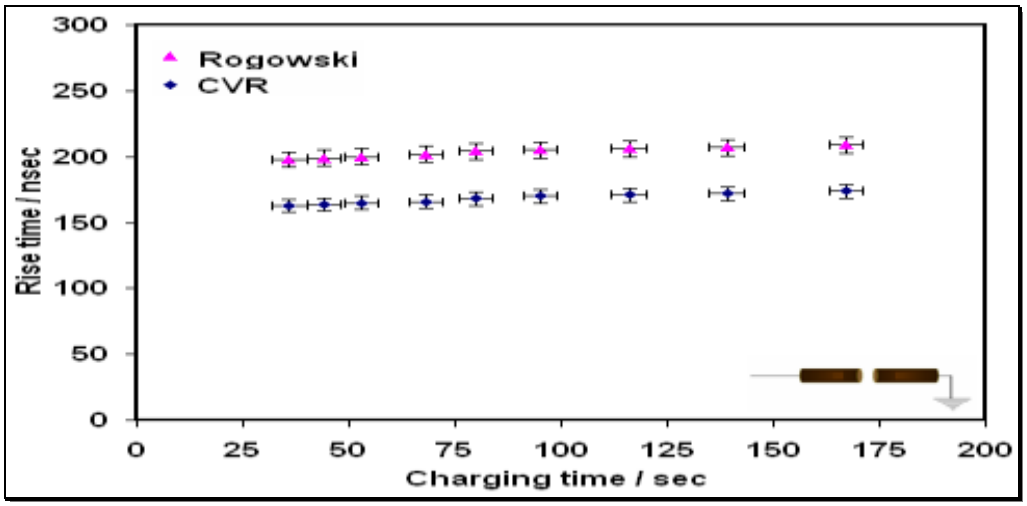

Figure 7-Rise time of the pulse as a function of charging time for Self-breakdown triggering.

Under these conditions when the dimensions of the electrodes are altered, both inductance (L) and capacitance (C) of the gap will be varied consequently because both L and C are geometry-dependent. Such variation of both L and C of the gap will introduce a change in the total impedance of the circuit giving rise to an alteration in the rising and decaying parts of the pulsed discharge current signal. This may be understood by the ratios (L / R) of the circuit for the rise-time and (RC) for the time after the peak current toward the end of the signal tail.

Figure-8 represents the rise time of the triggering (third electrode) breakdown to the discharge current for the same distance.

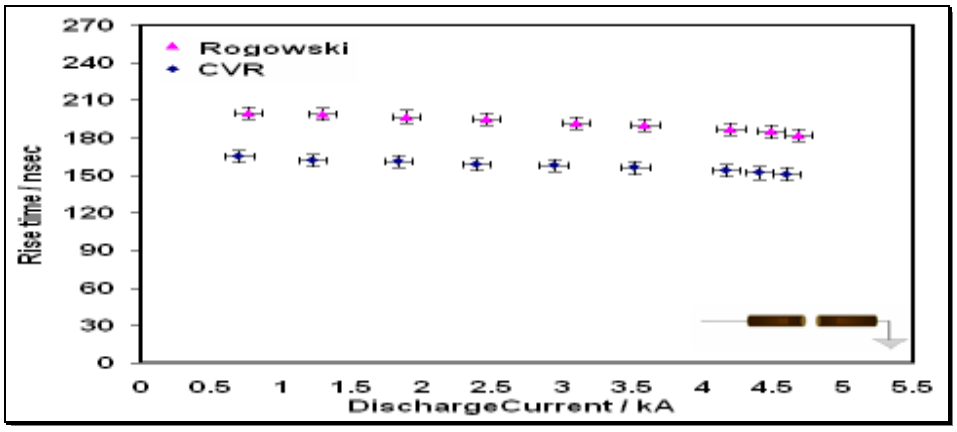

Figure 8- The rise time versus the discharge current for the same distance (d=2mm) by used third electrode triggering mode.

Taking the full-width at the half maxima of current signals obtained for gap spacing that ranged from 0.2 mm to 1.8 mm, a graphical representation demonstrates that the time required for short-circuiting the gap shows slight fluctuations as shown in Figure- 9. Such behaviour illustrates the effect of damping conditions created within the gap throughout the time interval of plasma expansion, i.e., oscillation conditions need more than time of full width at the half maxima (τ_{fwhm})to damp out for this circuit which is slightly underdamped.

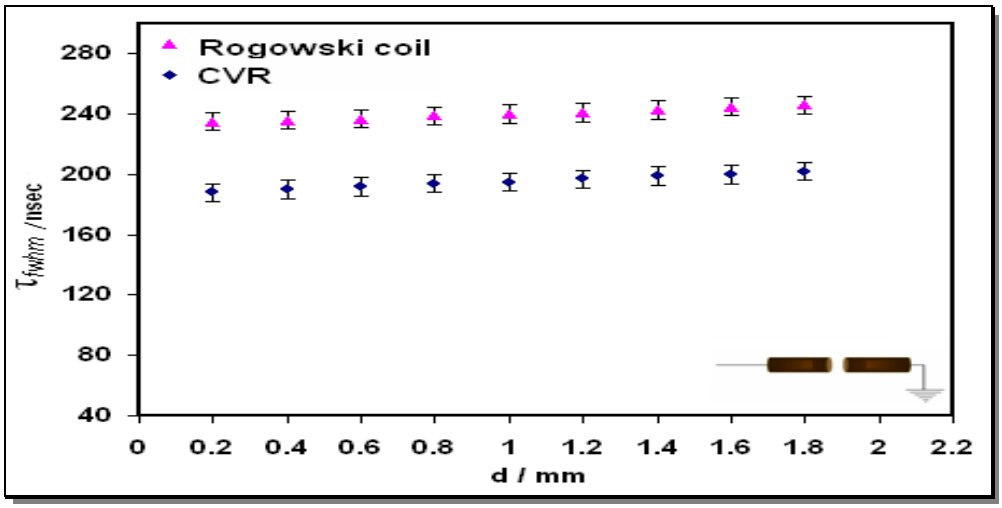

Figure 9- Variation of time of full width at the half maxima τ_{fwhm} with gap spacing.

3-3. Spatial Behaviors of the Spark Gap Voltage

The dependence of the breakdown voltage on the spark gap spacing is shown in Figure- 10 at small distance of (0.2, 0.4, 0.6, 0.8, 1, 1.2, 1.4, 1.6, and 1.8) mm. This behavior demonstrates that these experiments are run along the right side of the Paschen curve with a nonthermal plasma generated within the gap at atmospheric pressure. At this pressure, the plasma is highly conductive as spark ignition proceeds to arcing, which may impose a shrinkage of both normal and abnormal glow regions in the current –voltage characteristic curve of the discharge [29].

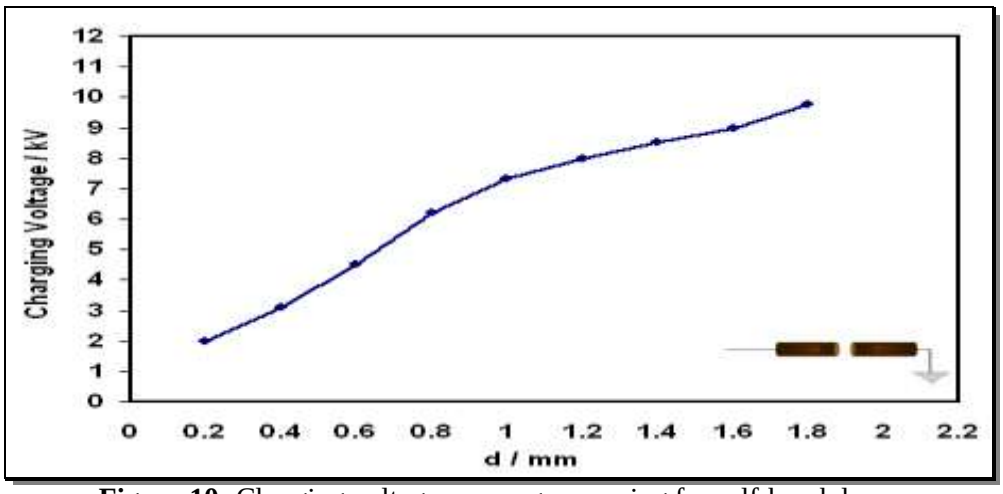

Figure 10- Charging voltage versus gap spacing for self-breakdown

3-4. Temporal Characteristics of the Impedance

A number of parameters were considered including the damping conditions, gap spacing and pulse duration. Two approaches were adopted to analyze the results of the output current signals. The first was to take a number of oscillograms for various gap spacing. A number of current values was extracted from each oscillogram that corresponds to a certain distance (d). For a number of d-values ranging from 0.5mm to 1.5 mm, the nominal impedance Z (charging voltage / discharge current) was plotted as a function of the rise time of each pronounced current peak on the oscillogram under self-breakdown conditions as shown in Figure- 11. The same trend of behaviour is obvious in both CVR and Rogowski coil measurements of the current as shown in Figure- 12. The values of Z increases with enlarging d while the impedance shows a prompt increase with rise time as a result of current degrading as the signal damps out due to the finite closure time of the spark gap. The peak current values showed a periodic damp out as a result of the behaviour of the external circuitry which must be accounted for in results analysis as will be discussed below. Typical value of Z for the resistance

(Figure 12a) took the range from 2.2 Ω to 80 Ω over a time period between 167 ns and 600 ns for a gap distance of typically 1.5 mm. Figure-12(b) shows a typical value of Z for the Rogowski coil taking a range from 2 Ω to 79 Ω over a time period between 205 ns to 620 ns and for a gap distance of typically 1.5 mm.

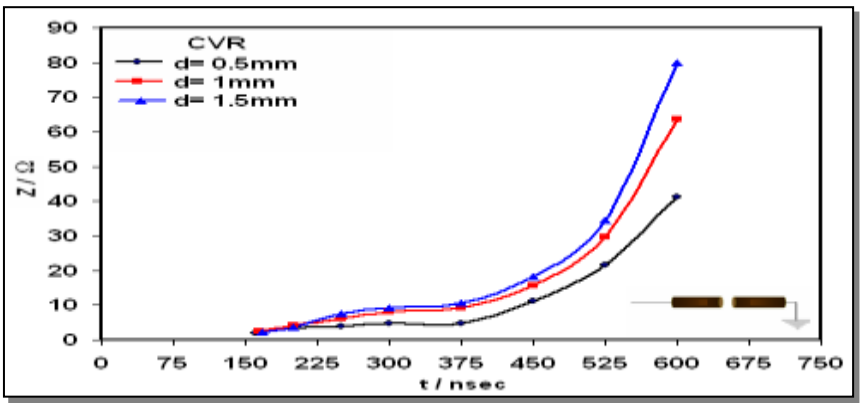

(a

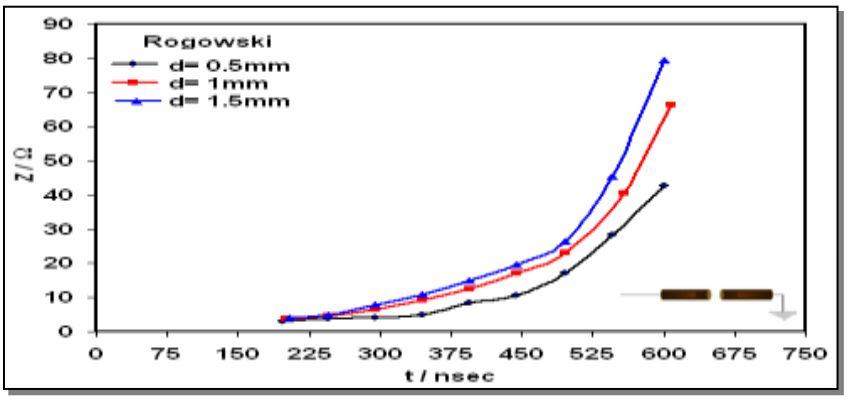

(b

Figure 11- Typical impedance behaviour for self-breakdown mode at different distance (a) CVR (b) Rogowski coil, extracted from various current oscillograms.

From a number of oscillograms the values of Z were obtained and plotted as function of the rise-time as demonstrated in Figure- 12.

It may be concluded from Figures- 11 and 12 that the time-evolution of Z depends on the inductance and resistivity of the spark gap as well as the expansion of plasma channels along the spacing d.

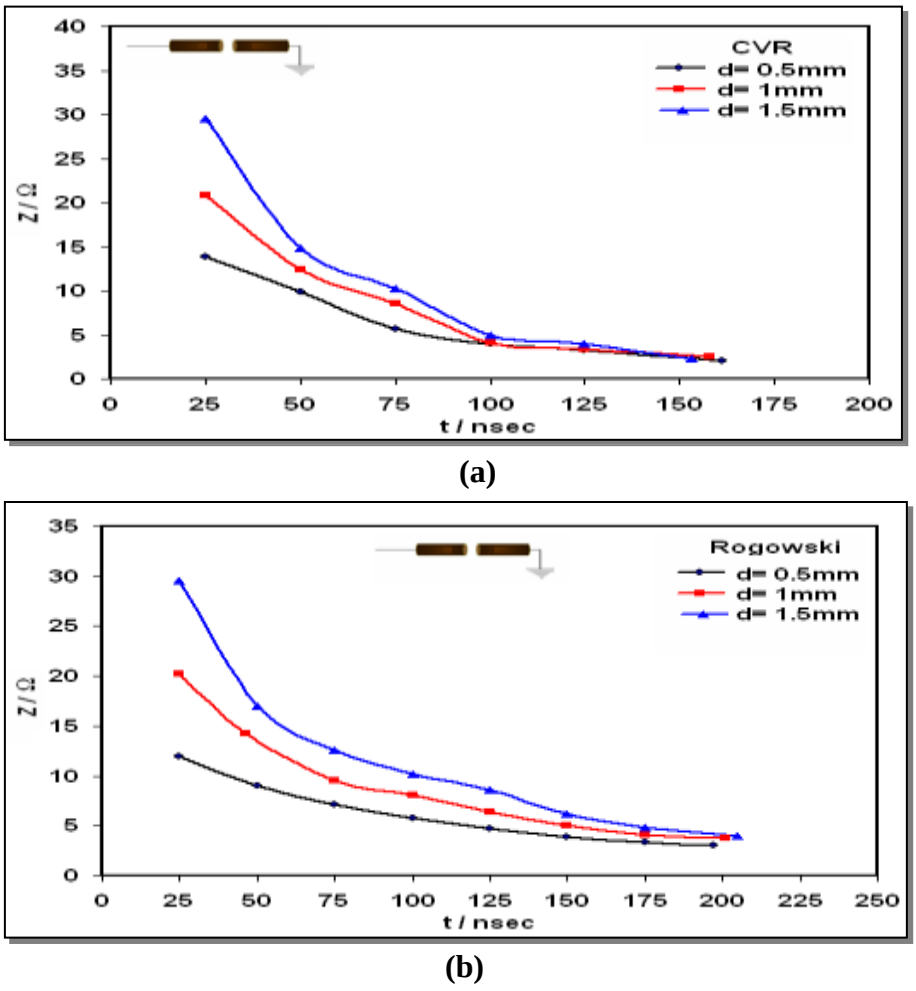

Figure 12- Impedance as a function of current rise- time for self-breakdown mode (a) CVR (b) Rogowski coil, extracted from various current oscillogram

The gap closure time may also be taken as the time required for the plasma to expand between the two gap electrodes resulting in an impedance collapse. Over the whole range of experimental conditions being undertaken, the average values of an overall nominal impedance were found in the range 2-30 Ω depending on the gap and circuit parameters. Also, this range implies the approximation of consider the charging voltage in the calculation.

4- Conclusion

Regardless of the complication of the physics behind the operation of pulsed plasma devices, these experiments have demonstrated a number of potentially practical conclusion, which can be summarized as follows:-

1. The temporal behaviour of the total circuit impedance showed a strong dependence on the behaviour of the nonthermal plasma which is generated during the breakdown process of the air between the spark gap electrodes.
2. All the discharge current waveforms showed damped oscillations from which results analyses were accomplished. These modes of oscillations may be governed by a dominating inductance in the circuit as well as the electronic components included in the methods of triggering.
3. The first cycle of the discharge current signal may be considered as that resulted from the spark gap closure by the plasma expansion the time of which is measured by the full width at the half maxima of this part of the signal.

4. Due to the existence of the external inductance in the circuit, damped pulses occur in the discharge current signals over a certain period of time which can be figured out from the RC time constant of each corresponding current signal.
5. The triggering method was found to have an effect on the discharge current pulses monitored by both current viewing resistance and Rogowski coil.

Reference

1. Hasaani, A. S., Ahmed, F. and Khdayeir, A. A. **2011**. Impedance Characteristics of Pulsed Atmospheric Electrical Discharge in Spherical Plasma Switch. *Baghdad Science Journal*, **8**(2): 630-637.
2. Esin, Bengisu Sozer **2008**. Gaseous Discharges and their Applications As High Power Plasma Switches for Compact Pulsed Powers Systems . MSc. thesis, University of Auburn.
3. Hasibur, Rahaman. **2007**. Investigation of a High Power, High Pressure Spark Gap Switch with High Repetition Rate. PhD. Thesis, University Erlangen–Nürnberg.
4. Meena, BL., Rai, SK., Tyagi, MS., Pal, UN., Kumar, M., and Sharma, AK. **2010**. Characterization of high power Pseudospark Plasma Switch (PSS). *Journal of Physics*: IOP Publishing , Conference Series 208, 012110 .
5. Hasibur Rahaman, Byung-Joon Lee, Jürgen Urban, Robert Stark, Klaus Frank and S.H. Nam .**2007**. A spark gap switch with very high repetition rate. 28th ICPIG, , Prague, Czech Republic. pp. 1496-1498, July 15-20 .
6. Horacio Bruzzone, Cesar Moreno and Roberto Vieytes. **1993**. Measurement of the time evolution of averaged impedances in small atmospheric pressure spark gap. *Meas. Sci. Technol*., **4:** 952 -956 .
7. Hasaani, S. **2010**. Correlation of Paschen Parameters in Magnetized argon Plasma. *Iraqi J. Phys*., 8(11): 95-101 .
8. Krasika, Ya. E., Chirko, K., Gleizer, J.Z., Krokhmal, A., Dunaevsky, A. and Felsteiner, J. **2002**. Application of a ferroelectric plasma cathode as a high-current switch. *Eur. Phys. J. D,* **19**: 89-95.
9. Frey, W., Sack, M. Wuestner, R. and Mueller. G. **2008**. Gas-Insulated Self-Breakdown Spark Gaps. Conference on Electrostatic Precipitation, pp.704-708.
10. Beveridge, J. R., MacGregor, S. J., Given, M. J., Timoshkin, I. V. **2009**. A Corona-stabilized Plasma Closing Switch. IEEE Trans. *Dielectr. Electr. Insul*., **16**(4): 948-955 .
11. Liu, Z.. Pemen, A. J. M., van Heesch, E. J. M. Yan, K., Winands, G. J. J., Pawlok, D. B. **2008**. A Multiple-switch Technology for High-power Pulse Discharging. 11th International Conference on Electrostatic Precipitation, pp.704-708.
12. Doucet, H.J., Roche, M., and Buzzi, J.M. **1988**. Very high Power Plasma Switches Basic Plasma and Switch Technology. 14, International congress on electric contacts Paris (FR), pp. 1-24.
13. Shaomao, Li. **2010**. Cold Cathode Materials for Pseudospark Switches. M.Sc., Thesis, Auburn University, Alabama .
14. Bluhm, H. **1996.** *Pulsed Power Systems: Principles and Applications*. Springer, Berlin.